

The Effective Spectral Resolution of the WFC and HRC Grism

A. Pasquali, N. Pirzkal, J.R. Walsh, R.N. Hook, W. Freudling, R. Albrecht, R.A.E. Fosbury
March 7, 2001

ABSTRACT

We present SLIM simulations of the WFC and HRC grism, obtained by varying the object size and orientation with respect to the dispersion axis. Our aim is to quantify the extent by which the object extension along the dispersion axis can degrade the nominal spectral resolution of the grism. We find that the line blending becomes significant for object diameters larger than 2 pixels and object major axis orientations $PA < 45^\circ$ with respect to the dispersion axis. As expected, the spectral resolution of the ACS grism decreases by almost a factor of two as the object size doubles.

Introduction

In the past 10 years, HST has featured a number of spectrographs working from UV to near IR wavelengths. Spectroscopy has been performed mostly through slits but the FOC, and more recently NICMOS and STIS, have also been used in slitless mode. Indeed, STIS parallel data are acquired through the G750L grating and without a slit at a spectral resolution of $4.9 \text{ \AA}/\text{pix}$ coupled with a spatial sampling of $0.051''$ per pixel. With the 2001 servicing mission, HST will also be able to perform spectroscopic observations with Advanced Camera for Surveys (ACS). In this case, observers will deal with grism and prism spectroscopy from 1150 \AA to 11000 \AA in combination with a spatial resolution ranging from $0.05''/\text{pix}$ (Wide Field Channel) to $0.032''/\text{pix}$ (Solar Blind Channel) and $0.027''/\text{pix}$ (High Resolution Channel). Since no slits are available in ACS, point

sources are expected to provide the best spectral resolution which is set by the instrument PSF and the pixel scale. In the case of ACS, the nominal spectral resolution is 40 Å/pix and 29 Å/pix in the first order spectra of the WFC and HRC grism, respectively. In the case of extended sources, their size, shape and orientation on the sky will inevitably degrade the ACS grism resolution.

We have explored the dependence of the ACS spectral resolution on the object size and orientation on the sky by means of spectroscopic simulations performed with the ST-ECF SLIM code (Pirzkal et al. 2001). The results obtained for the WFC and the HRC grism are presented in the following sections.

The ACS spectroscopic layout

Here, we briefly summarize the spectral elements deployed in ACS:

- the WFC (FOV = 3'.4 x 3'.4 at a spatial resolution of 0.05"/pix) is equipped with a grism covering the spectral range from 5500 Å to 11000 Å with a response peak at 7200 Å and 6000 Å in the 1st and 2nd orders, respectively. The grism dispersion is nearly linear and the resolving power is ~100, more specifically 40 Å/pix in the 1st order and 20 Å/pix in the 2nd order. The tilt of the spectra is nearly 2° with respect to the image X axis.
- The HRC (FOV = 30" x 30" with a spatial resolution of 0.027"/pix) uses the same grism, although the tilt of the spectra of 45° (with respect to the image X axis) increases the dispersion to 29 Å/pix in the 1st order and to 15 Å/pix in the 2nd order. The HRC also features a prism covering the 2000 - 5000 Å range, with a non linear resolution varying from 2.6 Å/pix at 1600 Å to 91 Å/pix at 3500 Å and 515 Å/pix at 5000 Å.

The SLIM simulations for the WFC

Two parameters can degrade the spectral resolution of a grism used without a slit: namely the object size, and for non-round sources, their size in the dispersion direction as set by their orientation.

We have explored these effects by simulating the spectrum of the Galactic Planetary Nebula NGC 7009, since the wealth of emission lines in their spectra makes Planetary Nebulae (PNe) standard wavelength calibrators. The NGC 7009 spectrum is a model spectrum derived from ground based and IUE observations. For the simulations, we have scaled the observed spectrum of NGC 7009 by a factor of 30 in flux to avoid CCD saturation in 1 second exposure time. Therefore, the line flux of Hβ has been decreased from 1.9×10^{-10} to 6.3×10^{-12} ergs cm⁻² s⁻¹. The resulting, scaled spectrum of NGC 7009 is shown in Figure 1 at a resolution of 0.5 Å/pix over the spectral range of the WFC grism. In this interval, its most prominent emission lines are HeI λ5876, Hα, [ArIII] λ7136 and

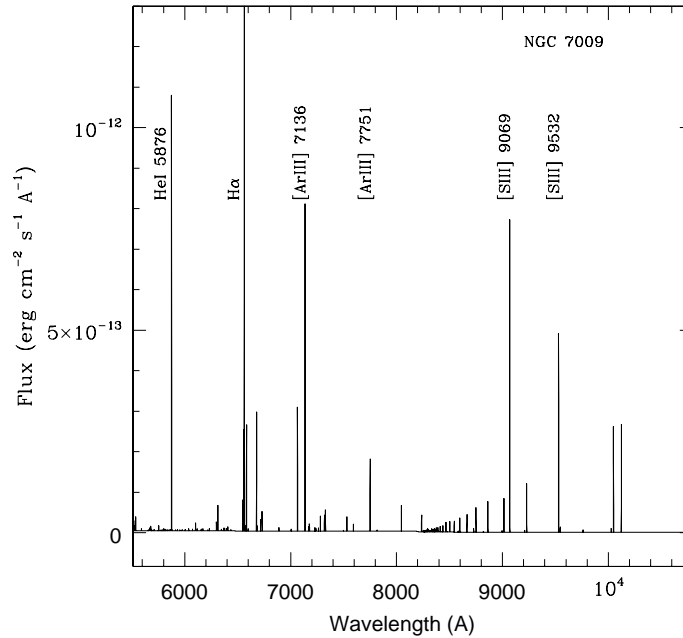


Figure 1: The scaled, model spectrum of the Galactic Planetary Nebula NGC 7009 with a spectral resolution of 0.5 Å/pix .

[SIII] $\lambda\lambda 9069, 9532$ lines. For the first run of the simulations, we have assumed the object to be a disc of variable, intrinsic size: from point source (PSF FWHM= $0.05''$ in the F606W filter selected for simulating direct images) to $0.1'' \times 0.1''$, $0.4'' \times 0.4''$ and $1'' \times 1''$. It has to be specified that the PSF used by SLIM version 1.0 is a Gaussian function whose FWHM value is set by the HST diffraction limit at any specific wavelength.

The simulated spectra have been extracted with the IRAF/APALL task by summing all the pixels in the cross-dispersion direction over which the flux is distributed. The 1st order spectra are plotted in Figure 2 in units of counts (SLIM agrees within 1% with the ACS spectroscopic ETC) and pixels from the object x-position in the direct image. The brightest emission lines have also been identified in Figure 2 as well as in Figure 3 where we have plotted the 2nd order spectra. No background or noise has been added to these simulations. For both orders, the line blending becomes severe at an object diameter $> 0.1''$ and grows quickly worse for more extended sources.

To quantify this, we have measured the FWHM of few non-blended lines in the 1st and 2nd order spectra of Figures 2 and 3; the values in Å are listed in Tables 1 and 2 with an uncertainty of $\sim 5\%$.

For the second run of the simulations, we have assumed the object to be elliptical, 0.1" x 0.25" in size, with the major axis oriented at different PA values (90° , 45° , 20° and 0°) from the image X axis. This means that for $PA = 90^\circ$ the object major axis is perpendicular to the image X axis, while at $PA = 0^\circ$ it is aligned along the image X axis. Once again, the exposure time employed for the simulations is 1 second and no background has been added to the simulated spectra. These have again been extracted with the IRAF/APALL task by summing all the pixels in the cross-dispersed direction over which the flux is distributed. The 1st order spectrum is shown in Figure 4.

As the object major axis gradually aligns with the dispersion axis, the line blending increases at $PA < 45^\circ$. This is reflected by the increase of the FWHM of some emission lines, that we have measured in the 1st and 2nd order spectra respectively (cf. Tables 3 and 4).

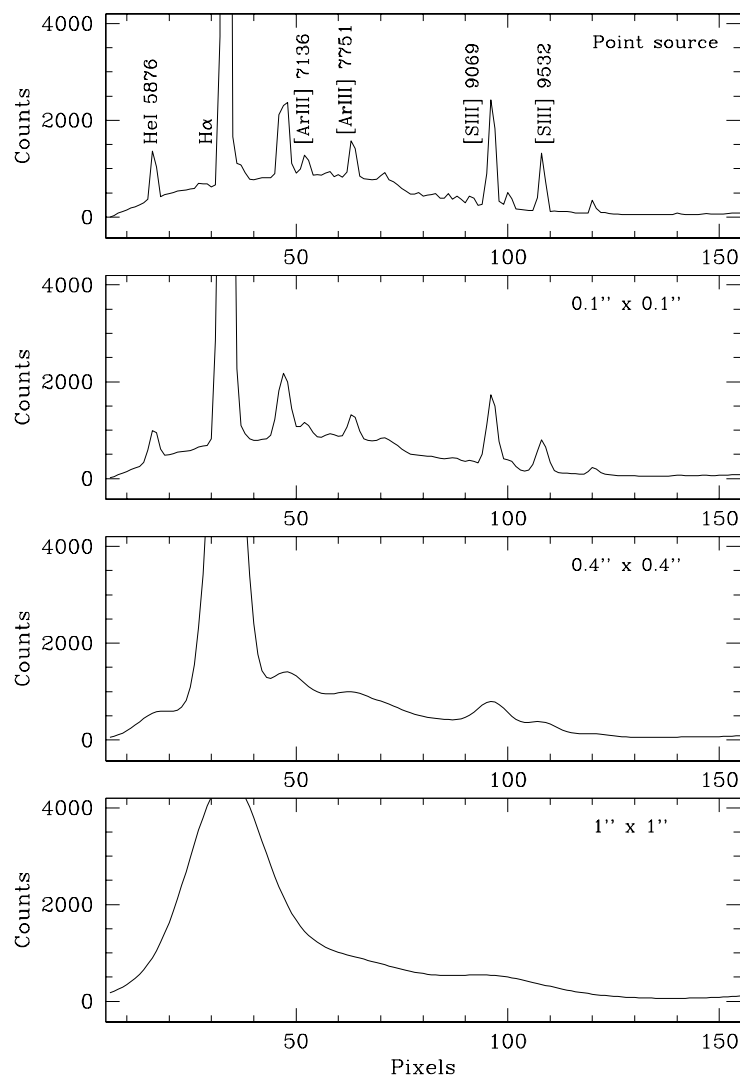


Figure 2: SLIM, 1st order spectra of NGC 7009 which have been obtained for the grism of the ACS WFC by increasing the object size. The adopted object shape is a disc and exposure time is 1 second. The nominal spectral resolution is ~ 40 Å/pix.

Lines	Point source	0.1'' x 0.1''	0.4'' x 0.4''
<i>1st order</i>			
HeI 5876	43 Å	84 Å	215 Å
[ArIII] 7751	57 Å	90 Å	-
[SIII] 9532	56 Å	103 Å	209 Å

Table 1. FWHM values of non-blended lines as a function of object size (a disc) for the 1st order spectra of the WFC grism.

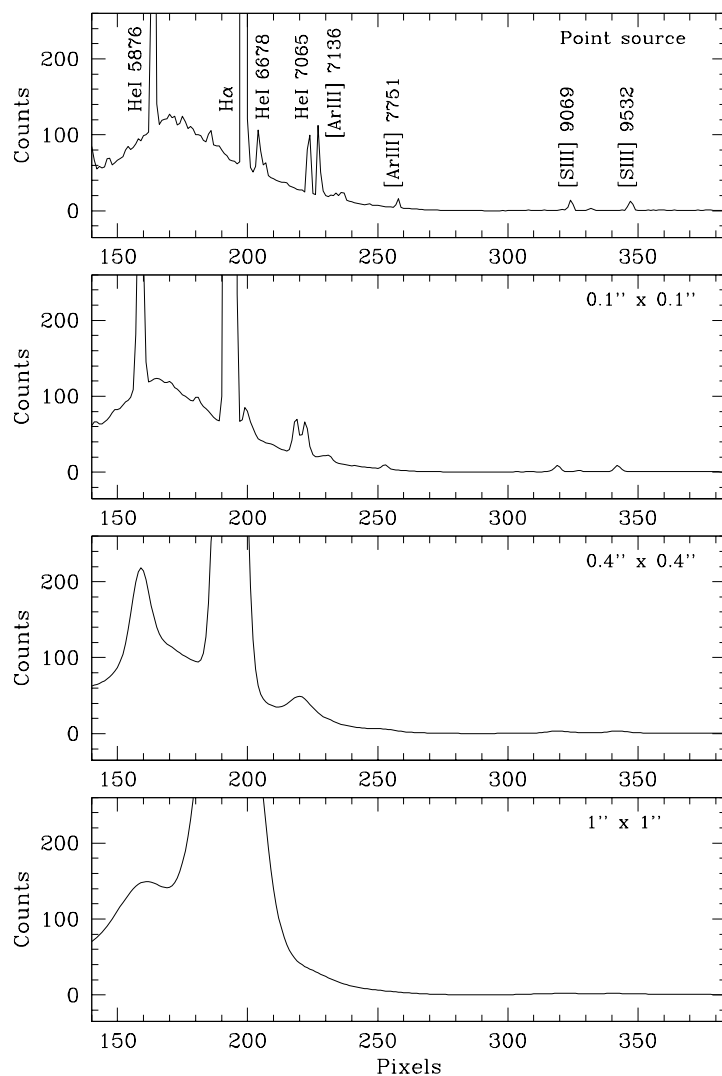


Figure 3: SLIM spectra of NGC 7009 as Figure 1 but for the 2nd order. The nominal spectral resolution is $\sim 20 \text{ \AA/pix}$.

Lines	Point source	0.1'' x 0.1''	0.4'' x 0.4''
<i>2nd order</i>			
HeI 5876	19 \AA	45 \AA	164 \AA
[SIII] 9069	32 \AA	54 \AA	172 \AA
[SII] 9532	36 \AA	55 \AA	162 \AA

Table 2. The same as in Table 1, but for the 2nd order spectra of the WFC grism.

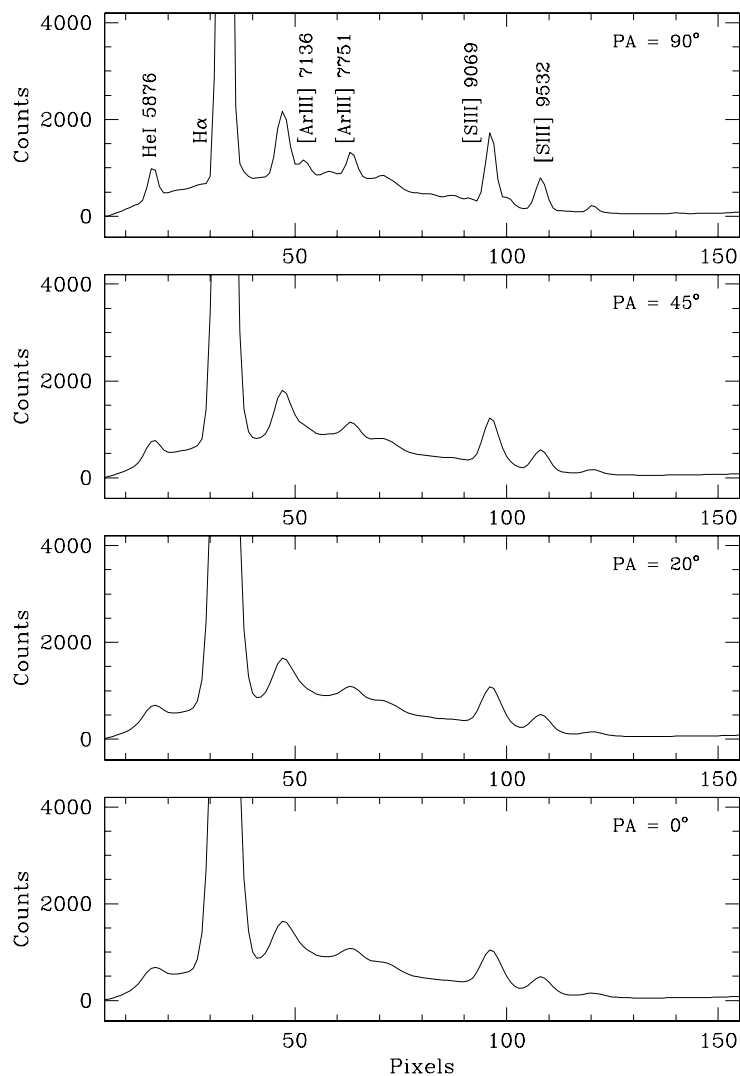


Figure 4: SLIM, 1st order spectra of NGC 7009 which have been simulated for the grism of the ACS WFC by rotating the object major axis of a 0.1'' x 0.25'' ellipse from perpendicular (PA=90°) to parallel (PA=0°) to the image X axis.

Lines	PA=90°	PA=45°	PA=0°
<i>1st order</i>			
HeI 5876	88 Å	143 Å	182 Å
[ArIII] 7751	96 Å	146 Å	189 Å
[SIII] 9532	111 Å	158 Å	189 Å

Table 3. FWHM values measured for non-blended lines as a function of object major axis orientation with respect to the dispersion axis, in the WFC grism images. The object shape is elliptical (0.1'' x 0.25'').

Lines	PA=90°	PA=45°	PA=0°
<i>2nd order</i>			
HeI 5876	44 Å	78 Å	104 Å
[SIII] 9069	55 Å	85 Å	111 Å
[SIII] 9532	56 Å	83 Å	105 Å

Table 4. The same as in Table 3, but for the 2nd order spectra of the WFC grism.

The SLIM simulations for the HRC

We have also applied the above procedure to the HRC grism simulations. The difference is that the object sizes have been scaled according to the smaller projected HRC pixel size (0.027"/pix in comparison with 0.05).

The spectrum of NGC 7009 has been simulated with 1 second exposure for round sources, whose diameter has been increased from point source (PSF FWHM=0.03" in the F606W filter selected for simulating direct images) to 0.06", 0.2" and finally 0.5". No background or noise has been added to the simulated spectra. The spectra have been extracted by: 1) rotating the grism image by 45° clockwise to align the dispersion axis with the image X axis; 2) adding up the rows in the spatial direction over which the spectra distribute.

The 1st order and 2nd order spectra are plotted in Figure 5 and Figure 6, respectively, in units of counts vs pixels from the object x-position in the direct image. The line blending becomes significant for an object diameter of 0.06" and quickly grows worse as the object size is increased to 0.5" x 0.5". This effect holds for both the orders. We have measured the FWHM of selected lines and the values in Å are given in Tables 5 and 6 for both the 1st and the 2nd order spectra of Figures 5 and 6.

Simulations have also been performed for the case of an elliptical source at various orientation with respect to the dispersion axis. For this specific application, we have assumed an object elliptical shape of 0.05" x 0.12" and projected the major axis at PA = 90° and 45° from the image X axis (or 45° and 0° with respect to the dispersion axis), with the same convention as for the WFC grism simulations. The simulated spectra have been extracted in the same way as above and the 1st spectrum is shown in Figure 7 in units of counts vs pixels from the object x-position in the direct image.

Tables 7 and 8 show the FWHM values determined for a sample of emission lines in both the 1st and 2nd order spectra as a function of the alignment of the object major axis.

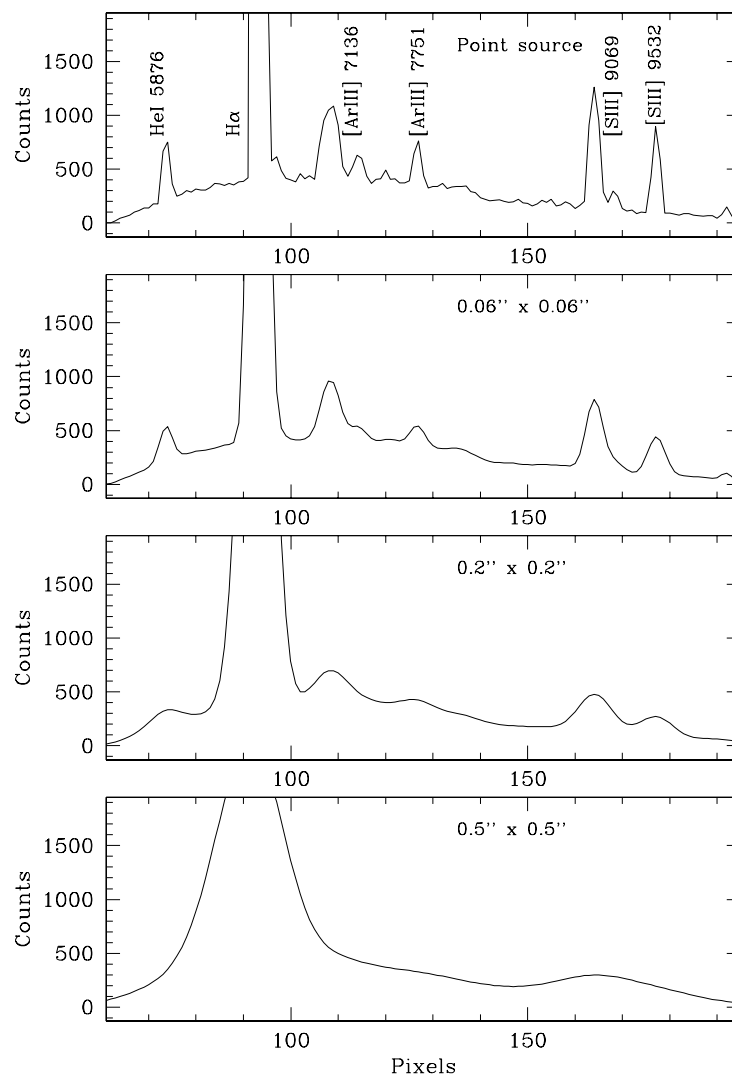


Figure 5: SLIM, 1st order spectra of NGC 7009 which have been computed for the grism of the ACS HRC by increasing the object size from a point source to 0.5'' x 0.5'' extended source. The object shape is a disc. The nominal spectral resolution is $\sim 29 \text{ \AA/pix}$.

Lines	Point source	0.06'' x 0.06''	0.2'' x 0.2''
<i>1st order</i>			
HeI 5876	51 Å	95 Å	198 Å
[ArIII] 7751	52 Å	104 Å	201 Å
[SIII] 9532	59 Å	126 Å	212 Å

Table 5. FWHM values measured for non-blended lines in 1st order spectra of the ACS HRC grism as a function of object size (a disc).

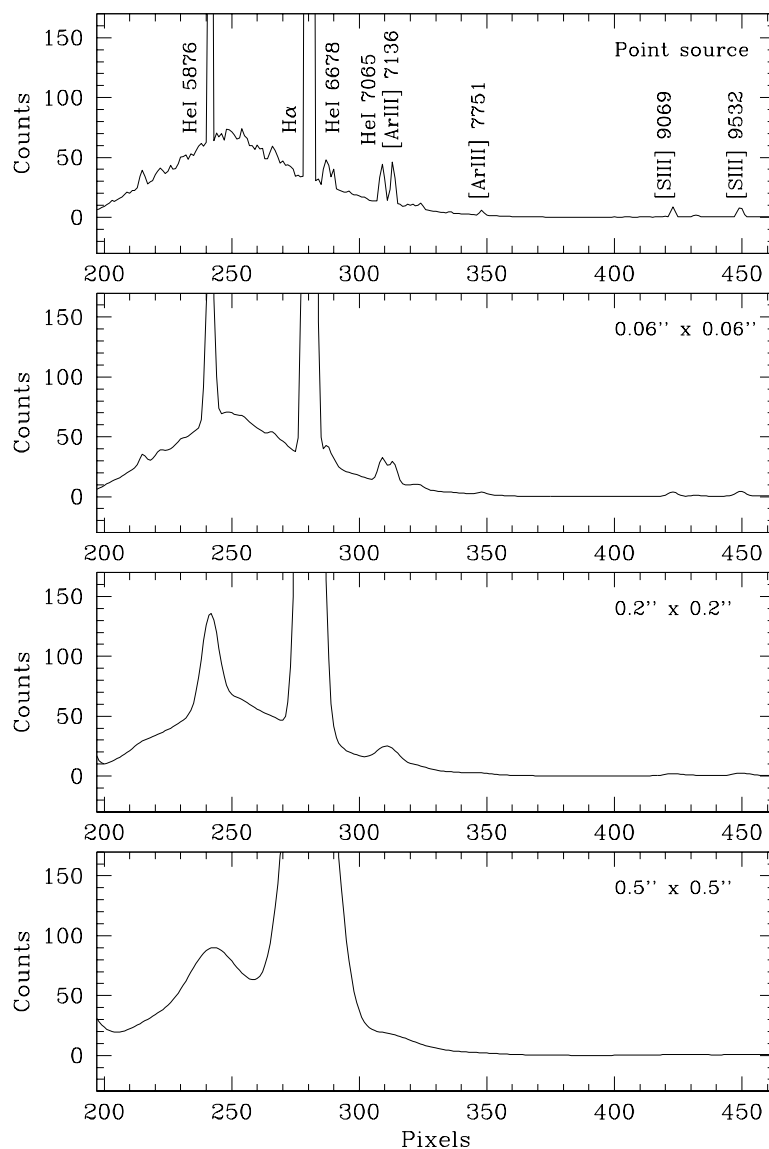


Figure 6: SLIM, 2nd order spectra of NGC 7009 for the ACS HRC for increasing object size from a point source to 0.5'' x 0.5'' extended source. The object is assumed to have a disc shape. The nominal spectral resolution is $\sim 15 \text{ \AA/pix}$.

Lines	Point source	0.06'' x 0.06''	0.2'' x 0.2''
<i>2nd order</i>			
HeI 5876	26 \AA	49 \AA	116 \AA
[SIII] 9069	27 \AA	67 \AA	126 \AA
[SIII] 9532	31 \AA	66 \AA	125 \AA

Table 6. The same as in Table 5, but for the 2nd order spectra of the HRC grism.

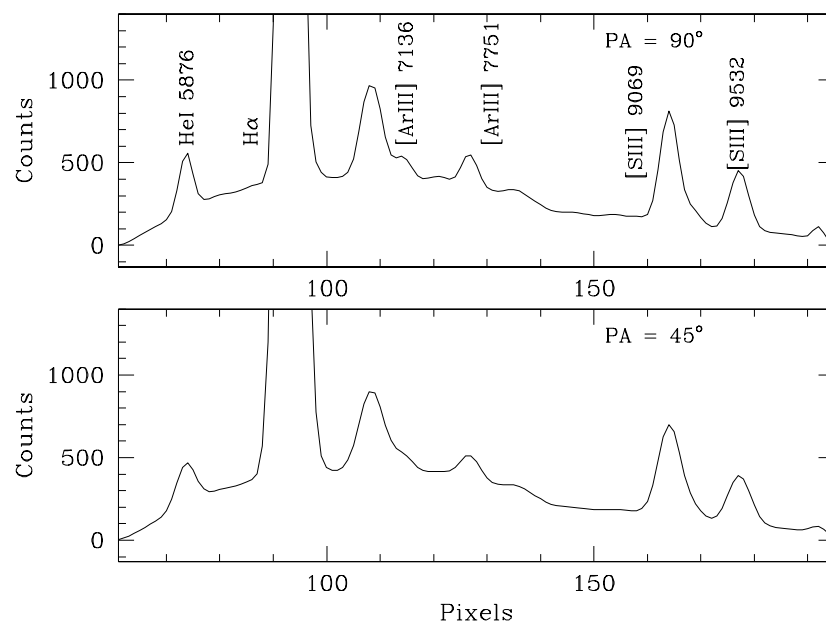


Figure 7: SLIM, 1st order spectra of NGC 7009 which have been simulated for the grism of HRC by orienting the object major axis at PA=90° and PA=45° with respect to the image X axis.

Lines	PA=90°	PA=45°
<i>1st order</i>		
HeI 5876	116 Å	141 Å
[ArIII] 7751	123 Å	146 Å
[SIII] 9532	147 Å	161 Å

Table 7. FWHM values of non-blended lines as a function of object major axis PA, in the HRC grism images. The object shape is elliptical (0.05'' x 0.12'').

Lines	PA=90°	PA=45°
<i>2nd order</i>		
HeI 5876	62 Å	74 Å
[SIII] 9069	78 Å	85 Å
[SIII] 9532	76 Å	86 Å

Table 8. The same as in Table 7, but for the 2nd order spectra of the HRC grism.

Conclusions

We have shown, by simulating WFC and HRC grism spectra, that the grism resolution is affected by both the object size and orientation with respect to the wavelength axis. In particular, line blending becomes important for object diameters larger than two pixels and as the object major axis gradually aligns with the dispersion axis ($PA < 45^\circ$) for elliptical sources.

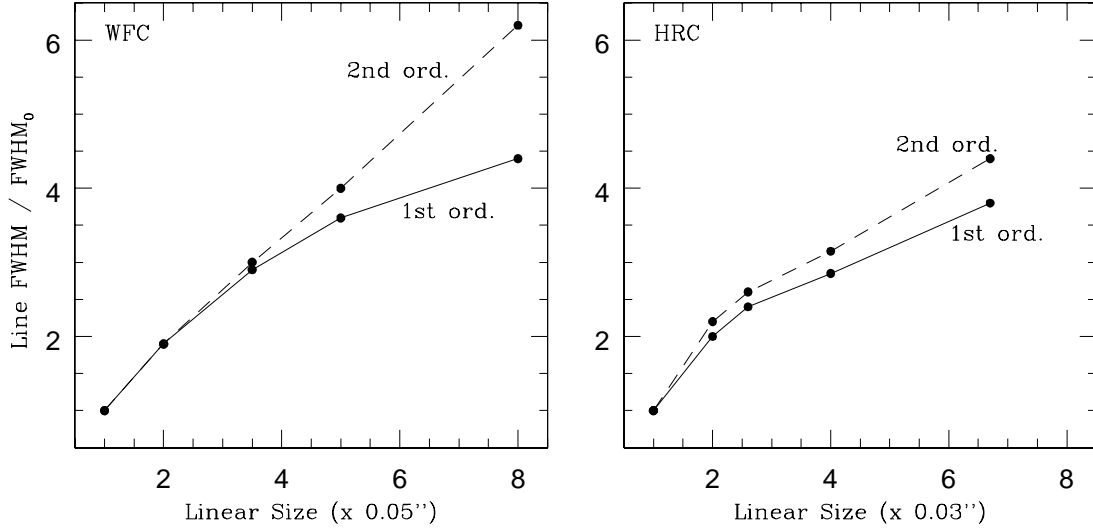


Figure 8: The spectral resolution of the WFC and HRC grism as a function of the object size. The solid line represents 1st order spectra and the dashed line corresponds to 2nd order spectra. The object diameter is plotted in abscissa as a multiple of the PSF FWHM in arcsec. The line FWHM is represented in the ordinate axis as a multiple of the mean FWHM in Å computed from the values of the lines in the point-source spectra: 52 Å for WFC 1st order, 29 Å for WFC 2nd order, 54 Å for HRC 1st order and 28 Å for HRC 2nd order.

As the PA of the major axis of an elliptical object (defined with respect to the dispersion axis) decreases, the projected, linear size of the object increases along the dispersion axis, degrading the spectral resolution in the same way as an increasing disc diameter. In the case of the WFC and an elliptical object 0.1'' x 0.25'' in size, the object extension along the dispersion axis increases from 0.1'' at $PA=90^\circ$, to 0.18'' at $PA=45^\circ$ and 0.25'' at $PA=0^\circ$, while for the HRC and an elliptical source 0.05'' x 0.12'' in size it grows from 0.08'' at $PA=90^\circ$ to 0.12'' at $PA=45^\circ$. We have merged these data with the spectra simulated for a disc of varying diameter into a final dataset, which correlates the line FWHM with the object extension along the dispersion axis. In particular, the object extension in the dispersion direction is expressed in units of the PSF FWHM of a point source, namely 0.05'' for the WFC and 0.03'' for the HRC (as measured on the simulated direct images, whose ref-

erence filter is F606W). The line FWHM values are normalized to those measured for a point source in the grism images of both the WFC and the HRC: 52 Å and 29 Å for the WFC 1st and 2nd order spectra, 54 Å and 28 Å for the HRC 1st and 2nd order spectra. This dataset is plotted in Figure 8. The left panel represents the trends for the WFC 1st and 2nd order grism spectra, with solid and dashed lines respectively. The right panel is the same, but for the HRC 1st and 2nd order spectra. Within the uncertainty (~5%) of the line FWHM measurements, the line FWHM nearly doubles with a doubling of the object extension, particularly in the 2nd order which has a higher spectral resolution. This is true for both the WFC and the HRC; the grism spectral resolution degrades by almost the same factor as the object size increases.

It has to be specified that the above results have been obtained from simulated spectra, background free and extracted with the box option. The presence of background and noise, although worsening the S/N ratio of data, may reduce the useful object size in the cross-dispersion direction and hence necessitate a smaller height of the extraction aperture. Also, an extraction algorithm which uses an aperture tilted as the object major axis PA would help in partially recovering the nominal spectral resolution of the ACS grism. None of the above, however, affects the object extension in the wavelength axis which remains the primary constraint on the effective spectral resolution of the ACS grism.

We present in Figure 9 a realistic simulation of the Planetary Nebula #31 in Andromeda (Ciardullo et al. 1989) as acquired with the WFC grism. For this simulation, we have adopted the model spectrum of NGC 7009 and scaled it by the H β flux ratio between NGC 7009 [LogF(H β)=-9.7] and PN #31 [LogF(H β)=-14.6]. NGC 7009 has a linear size of ~0.05'' at the distance of Andromeda (730 Kpc), therefore we have assumed a point source for its simulation. We have integrated for 1200 seconds and added to the grism image a Poisson background of 191 counts/pix according to the STScI ACS Exposure Time Calculator. No intrinsic (e.g. stellar) background has been considered in this simulation, which would exist when Planetary Nebulae in a distant galaxy are observed (except halo objects). The output 1st and 2nd order spectra have been extracted with a box 0.6'' (12 pixels) in height.

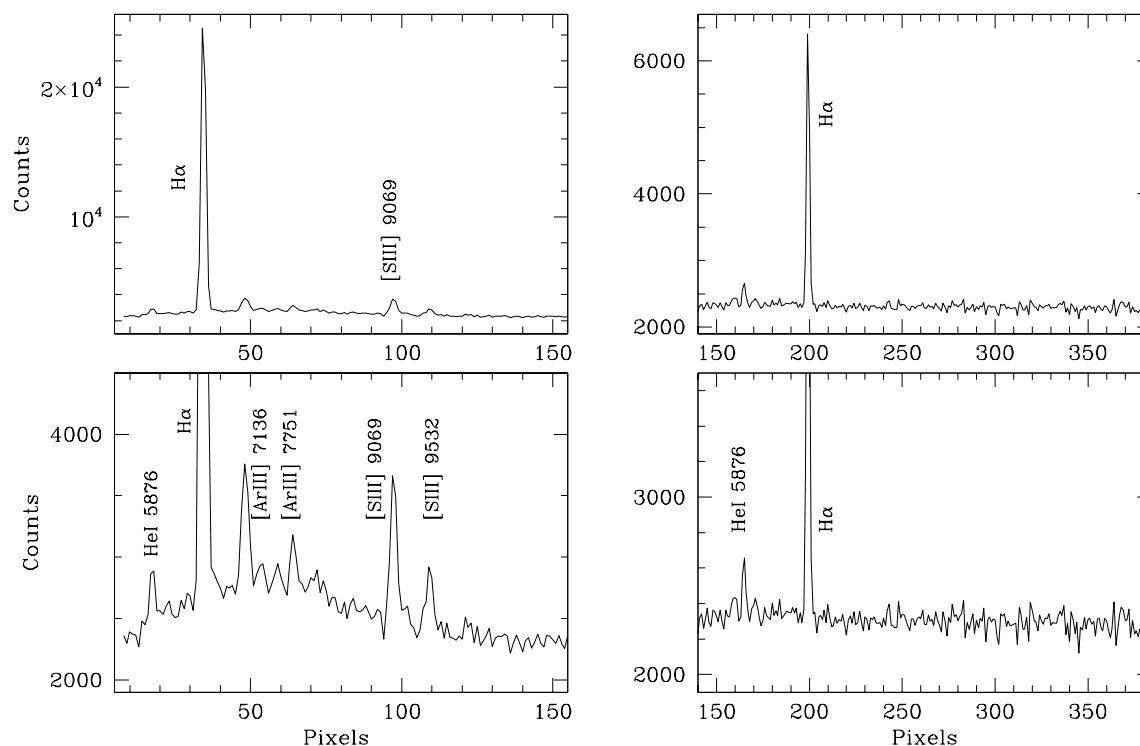


Figure 9: A realistic simulation of the Planetary Nebula #31 in Andromeda (Ciardullo et al. 1989) as observed with the WFC grism. The upper panels plot the 1st (left) and 2nd order (right) spectra respectively at their full flux scale. The bottom panels offer a close-up on the fainter emission lines in the 1st (left) and 2nd (right) spectra, respectively. The exposure time is 1200 seconds and the background appropriate for this exposure time was added.

References

Ciardullo, R., Jacoby, G.H., Ford, H.C., Neill, J.D., 1989, ApJ, 339, 53

Pirzkal, N., Pasquali, A., Walsh, J.R., Hook, R.N., Freudling, W., Albrecht, R., Fosbury, R.A.E., 2001, “ACS Grism Simulations using SLIM 1.0”, ST-ECF ISR ACS 2001-001